https://doi.org/10.18321/ectj821

Study of Luminescence in Noble Gases and Binary Kr-Xe Mixture Excited by the Products of ^{6}Li(n,α)T Nuclear Reaction

K. Samarkhanov[1]*, E. Batyrbekov[2], M. Khasenov[3], Yu. Gordienko[1], Zh. Zaurbekova[1], V. Bochkov[1]

[1]Branch Institute of Atomic Energy, NNC of RK, 10 Krasnoarmeyskaya str., Kurchatov, 071100, Kazakhstan
[2]National Nuclear Center of RK, 2 Krasnoarmeyskaya str., Kurchatov, 071100, Kazakhstan
[3]National Laboratory Astana, 53 Kabanbay Batyr Ave., Astana 010000, Kazakhstan

Article info

Received:
4 September 2018

Received in revised form:
15 November 2018

Accepted:
26 December 2018

Keywords
Nuclear-excited plasma
Lithium
Noble gases
Reactor irradiation
Ampoule device

Abstract

At the present time the direct nuclear energy conversion into optical radiation is realized in gas media in which filling of energy levels takes place in the low-temperature plasma (nuclear-excited plasma) induced by ionizing radiation. The research of optical radiation of the nuclear-excited plasma induced by products of nuclear reactions is interest for development of an alternative outlet method of energy from the nuclear reactor, creation of control and regulating bodies for parameters of nuclear reactors as well as creation of one of diagnostics of high-temperature plasma in fusion reactors. The purpose of this work was to obtain new experimental data about processes of nuclear energy conversion into optical radiation with the optimal gas media having high coefficient of nuclear energy conversion into optical radiation and also with a possibility of outlet method of energy from the nuclear reactor core. In this article, description of the reactor experimental bench (LIANA) and the experiment scheme, the irradiating ampoule device (AD) with surface source of charged particles is provided, and the procedure of reactor experiment is presented. This paper presents the results of the reactor experiments of studying the spectral-luminescent characteristics of unary noble gases (Ne, Ar, Kr, Xe) and binary Kr-Xe gas mixture in a 200–975 nm spectral range with ionization gaseous media by products of ^{6}Li(n,α)T nuclear reaction under irradiation at research water-cooled heterogeneous reactor (the IVG.1M).

1. Introduction

The efficiency of converting nuclear energy into light energy depends largely on the choice of the active gaseous media excited by nuclear reaction products [1]. If a suitable composition of the gaseous media is found, then it is possible to ensure selective level filling of impurity gas in these collisions where laser generation can be obtained [2]. Efficient excitation of the gaseous media needs isotopes interacting with neutrons in direct contact with this gaseous media. At various times, exothermic neutron nuclear reactions such as ^{3}He(n,p)T, ^{10}B(n,α)^{7}Li and ^{235}U(n,f)F were used to generate a nuclear-excited plasma.

The Branch of Institute of Atomic Energy of National Nuclear Center of RK (Kurchatov, Kazakhstan) is currently conducting the experiments on studying the spectral-luminescent properties of a nuclear-excited plasma induced by nuclear reaction products of ^{6}Li(n,α)T, by using surface sources of charged particles.

2. Experimental facility and technique of reactor experiments

2.1. Experimental bench

The reactor experiments on studying the luminescence spectra of gaseous media was held on the LIANA experimental bench, located in a stationary reactor hall, at a flux of thermal neutrons of $1.44 \cdot 10^{14}$ n/(cm^{2}s) [3]. Figure 1 shows a schematic diagram of the LIANA experimental bench.

*Corresponding author. E-mail: samarkhanov@nnc.kz

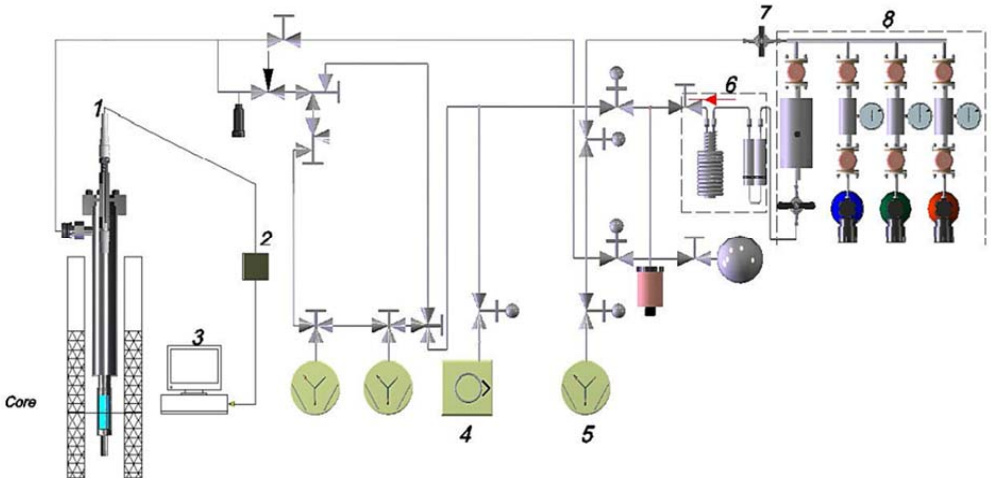

Fig. 1. A schematic diagram of the modernized LIANA experimental bench: 1 – ampoule device; 2 – optical spectrometer; 3 – PC; 4 – fore vacuum pump; 5 – high-vacuum pump; 6 – palladium-silver filter; 7 – stop valves; 8 – tank with spectrally pure gas.

The LIANA experimental bench was initially intended for carrying out researches of hydrogen isotopes interaction in metals and alloys at the various temperatures of a sample and inlet pressures of gases, including at the influence of reactor irradiation (detailed description of LIANA experimental bench is provided at [4, 5]).

The experimental bench consists of an ampoule device (1) and a working unit. The working unit consists of a vacuum system, a system for purification (6), information and measuring complex. The vacuum system consists of fore vacuum (4) and high vacuum parts (5), connected by the pipelines with the stop valves (7). Under the influence of neutron flux from the IVG.1M reactor, lithium as fissionable material emits charged particles (He and ^{3}H) which excite the gas medium that leads to its luminescence. The luminescent radiation gets into input of the collimator and focuses on input of the optical fiber cable. Transmitted luminescent radiation through the cable goes to input of a QE65 Pro-abs optical spectrometer (2) and is recorded as a luminescence spectrum on the hard disk of PC (3).

2.2. Experimental ampoule device

For the reactor experiments on studying the spectral-luminescent properties of noble gases and their binary mixtures under conditions of reactor irradiation, a special ampoule device (AD) with an experimental cell was designed. Figure 2 shows a schematic design, 3D-view and the main elements of the AD.

As fissionable material, lithium with enrichment by ^{6}Li – 7.5% with a layer thickness 0.05 mm and high 150 mm was used. The procedure for applying a thin layer of lithium on the inner side of the experimental cell of AD is described in [6].

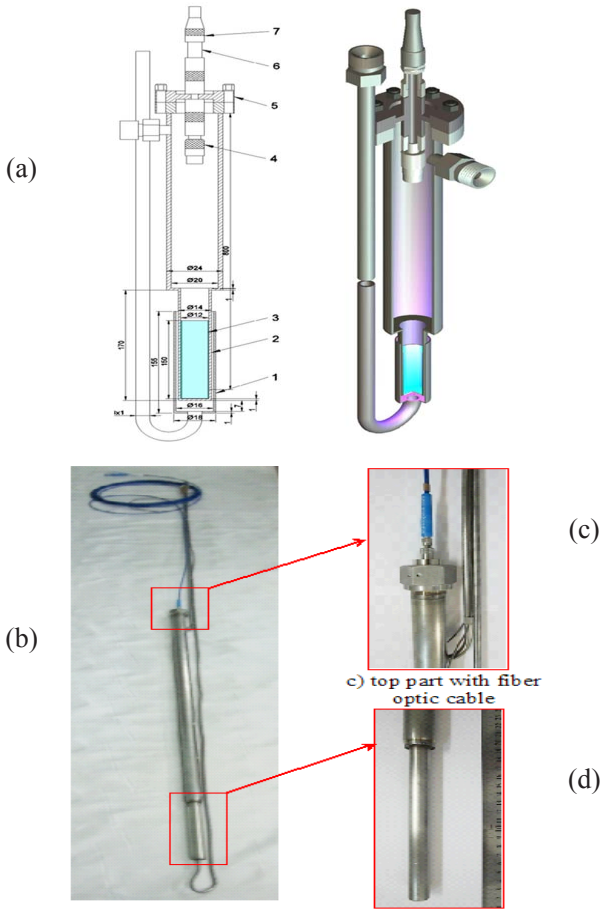

Fig. 2. Ampoule device based on noble gases: (a) – schematic design and 3D-view: 1 – cooling shell; 2 – AD body; 3 – lithium layer; 4 – optic collimator; 5 – flange; 6 – optic adapter; 7 – optic cable; (b) – general view of AD with cooling shell; (c) – top part with fiber optic cable; (d) – experimental cell of AD.

Materials of AD, experimental cell and other component parts were made from 12Cr18Ni10Ti stainless steel. The dimensions of AD: 59 mm × 900 mm. The dimensions of the experimental cell: diameter 14 mm, length 170 mm. AD design allows "recharge" gaseous media during the reactor experiment.

2.3. Technique of the reactor experiments

In view of the technological features of the IVG.1M research reactor and LIANA experimental bench, a technique of reactor experiments on studying the spectral-luminescent properties of noble gases, excited by the products of ^{6}Li(n,α)T nuclear reaction has been developed, which consists in the following: AD was loaded in the experimental channel of the IVG.1M reactor. Thus, the center of experimental cell coincided with reactor core center. Hereafter, AD connected with the vacuum system of the experimental bench and all necessary technological procedures on preparation of loaded device and LIANA bench for reactor irradiation experiments were conducted. Then, prior to reaching the targeted level of the reactor power, the studied gases were supplied into the AD volume up to required pressure. After this, the reactor was set on the targeted level of power, luminescent spectrum of gaseous media, excited by the products of ^{6}Li(n,α)T nuclear reaction, appearing in the volume of the experimental cell of AD was recorded. After recording the luminescence spectra at targeted level of power of the IVG.1M reactor the pressure or composition of gaseous media changed. When luminescent spectrum of gas mixture at all studied stationary levels of reactor power were measured, the planned reactor shutdown was done.

3. Results and discussion

Several reactor experiments [6–8] were conducted at the LIANA experimental facility by the method described above.

The AD was heated through the radiation heating up of the steel pipe and the energy extraction in the lithium layer, the temperature was regulated by a change in the nitrogen flow rate with external cooling. The temperature of the outer surface of the tube with lithium was recorded with the help of two thermocouples which were located in the middle of the height of the lithium layer. The temperature of the experimental cell's walls was 313 K.

3.1. The results of experiments with unary noble gases excited by the products of ^{6}Li (n,α)T nuclear reaction

The first reactor experiment was conducted with neon noble gas. The volume of the ampoule device was degassed in the reactor core at 413 K and, before filling, purged several times with the studied gases with impurities less than 0.001%. Next, with the help of the puffing system, the studied gas was supplied by portions into the volume of the AD up to a pressure of 1 atm. Figures 3 and 4 show the spectrum of the neon emission with the background subtraction for different values of the integration time.

In the neon luminescence spectrum, the lines belonging to the *3p-3s* transitions of the neon atom dominate, and the *3d-3p* lines are also available in the IR area. In the near portion of the spectrum, there are bands of molecular nitrogen ions (391.4 nm, 427.8 nm, 471 nm), which is explained by the present of impurities. The obtained data are in good consistent with the results of other studies [9].

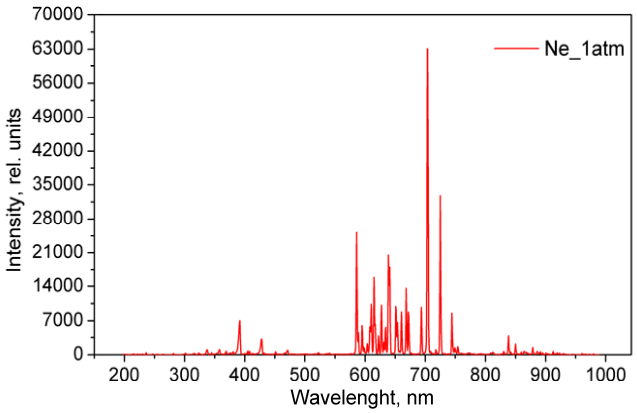

Fig. 3. Neon emission spectrum at τ = 300 ms.

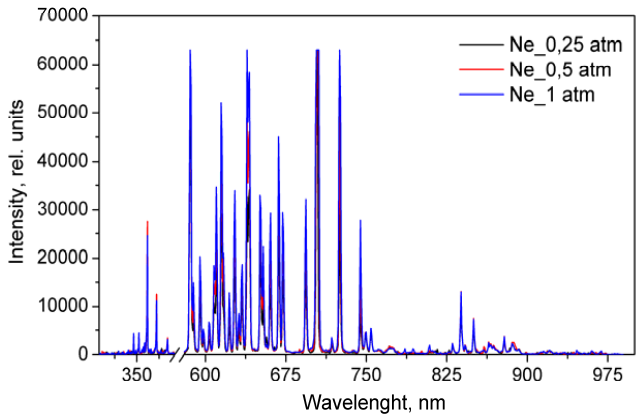

Fig. 4. Neon emission spectrum at τ = 1 s.

The presence of impurities is consistent with the results of other studies [10], in which intensive lines and impurity bands were recorded during ionizing radiation even in cases where high purity gases were used. Emission intensity distribution of separate lines of neon, in the wavelength range from 200 to 975 nm is presented in Table 1.

The intensity of the atomic lines appears in relative units without correction for the spectral sensitivity of the experimental setup.

Table 1

Emission intensity distribution of separate lines of neon

Wavelength measured, nm	Wavelength table, nm	Transition	0.3 s	1 s	3	10 s	Intensity, rel. units
391.9	391.4	$(B^2S_u^+)_{n=0} - (X^2S_g^+)_{n=0}$	7.0	24.5	hv	hv	245
427.7	427.8	$(B^2S_u^+)_{n=0} - (X^2S_g^+)_{n=1}$	3.1	10.9	33.9	hv	113
471.0	470.9	$(B_2S_u^+)_{n=0} - (X^2S_g^+)_{n=2}$	0.8	3.1	9.4	32.4	32
540.8	540.0	2p1-1s4	0.4	1.2	3.80	12.4	12
585.8	585.2	2p1-1s2	25.2	hv*	hv	hv	840
588.9	588.2	2p2-1s5	4.5	15.0	45.2	hv	151
594.9	594.4	2p4-1s5	6.2	20.5	61.0	hv	203
597.9	597.5	2p5-1s5	1.6	5.2	15.9	53.6	54
603.3	602.9	2p2-1s4	2.0	6.8	20.5	hv	68
607.8	607.4	2p3-1s4	5.5	18.4	55.2	hv	184
610.1	609.6	2p4-1s4	10.4	34.8	hv	hv	348
614.6	614.3	2p6-1s5	15.9	52.3	hv	hv	523
616.9	616.3	2p2-1s3	6.4	21.2	hv	hv	212
622.2	621.7	2p7-1s5	3.9	13.0	38.9	hv	130
626.7	626.6	2p5-1s3	8.1	29.9	hv	hv	270
631.3	630.5	2p6-1s4	2.6	8.6	25.5	hv	85
633.5	633.4	2p8-1s5	4.6	15.3	46.3	hv	154
638.8	638.3	2p7-1s4	20.5	hv	hv	hv	686
641.1	640.2	2p9-1s5	17.9	58.6	hv	hv	586
650.9	650.7	2p8-1s4	10.0	33.0	hv	hv	330
653.9	653.3	2p7-1s3	6.7	22.4	hv	hv	224
659.9	659.8	2p2-1s2	6.3	21.2	hv	hv	212
668.2	667.8	2p4-1s2	13.5	45.1	hv	hv	451
671.9	671.7	2p5-1s2	8.8	29.7	hv	hv	297
693.7	692.9	2p6-1s2	9.8	32.3	hv	hv	323
702.7	702.4	2p7-1s2	16.3	52.4	hv	hv	524
703.4	703.2	2p10-1s5	47.6	hv	hv	hv	1587
717.6	717.3	2p8-1s2	1.0	3.5	hv	hv	36
725.1	724.5	2p10-1s4	33.2	hv	hv	hv	1107
744.4	743.8	2p10-1s3	8.7	28.0	hv	hv	280
749.6	748.8	3d-3p	1.4	4.6	14.0	48.1	48
754.1	753.5	3d-3p	1.9	5.4	16.6	55.6	55
830.2	830.0	3d-3p	0.7	2.4	7.0	25.0	25
838.3	837.7	3d-3p	3.9	13.2	38.5	hv	128
841.9	841.8	3d-3p	0.6	2.2	6.1	21.0	21
850.0	849.5	3d-3p	2.2	0.7	22.3	hv	74
863.9	863.4	3d-3p	0.7	2.5	7.7	26.5	26
878.5	878.3	3d'-3p'	1.2	3.5	11.2	36.9	36
885.8	885.3	3d-3p	0.7	2.3	7.2	25.0	25

*hv – high value (i.e. off scale)

Table 2
Emission intensity distribution of separate lines of argon

Wavelength measured, nm	Wavelength table, nm	Transition	0.1 s	0.3 s	1 s	3 s	10 s	Intensity, rel. units
696.7	696.5	2p2-1s5	4.1	12.5	41.7	hv	hv	417
707.1	706.7	2p3-1s5	0.2	0.7	2.4	7.7	25.5	25.5
727.3	727.2	2p2-1s4	0.9	2.5	8.5	25.9	hv	86.3
738.5	738.3	2p3-1s4	0.4	1.2	4.2	12.5	41.4	41.4
750.4	750.3	2p1-1s2	1.6	4.8	16.2	48.7	hv	162
751.1	751.4	2p5-1s4	1.8	5.3	17.7	52.8	hv	176
763.7	763.5	2p6-1s5	5.9	17.8	59	hv	hv	590
772.6	772.4	2p7-1s5	7.5	22.8	hv	hv	hv	760
794.8	794.8	2p4-1s3	0.7	2.2	7.2	22.1	hv	74
801.5	801.4	2p8-1s5	1.1	3.4	11.3	34.4	hv	115
811.8	811.5	2p9-1s5	2.5	7.6	25.6	hv	hv	256
826.5	826.4	2p2-1s2	6.1	18.4	60.9	hv	hv	609
841.2	840.8	2p3-1s2	0.8	2.4	8	24.3	hv	81
842.7	842.4	2p8-1s4	1.4	4.3	14.5	43.5	hv	145
852.2	852.1	2p4-1s2	0.5	1.2	3.9	12	41.1	41.1
866.8	866.7	2p7-1s3	0.1	0.2	0.8	2.2	7.6	7.6
912.7	912.2	2p10-1s5	3.2	9.4	31.7	hv	hv	317
922.9	922.4	2p6-1s2	0.4	1.2	4.4	11.8	40	40
966.2	965.7	2p10-1s4	0.3	0.8	3	8.8	29.7	29.7

The condition for experiments with neon was similar to experiments with argon. The Figs. 5 and 6 show the argon luminescence spectra at different values of the integration time.

The argon emission spectra consist mainly of ArI lines that refer to the transitions of *4p-4s* of the argon atom. Emission intensity distribution of separate lines of argon is presented in Table 2.

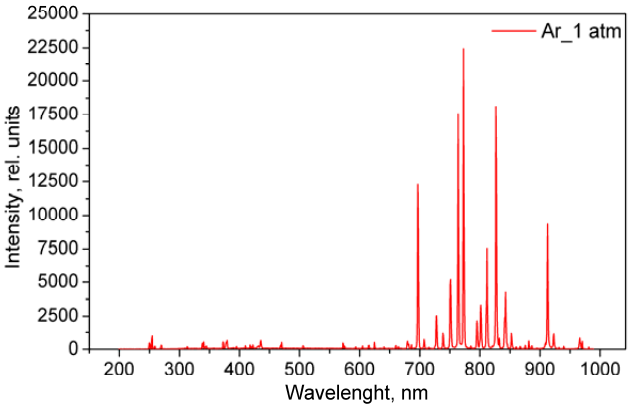

Fig. 5. Argon emission spectrum at τ = 300 ms.

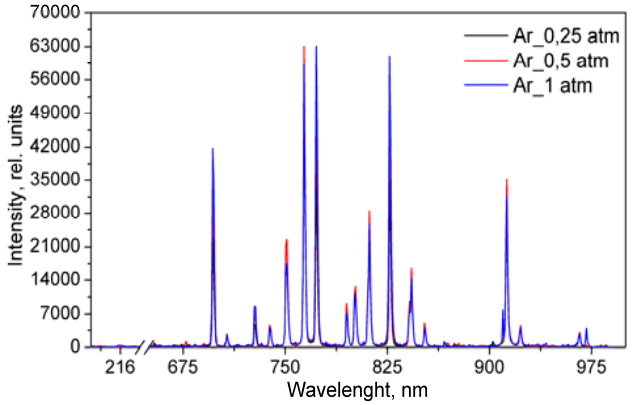

Fig. 6. Argon emission spectrum at τ = 1 s.

The conditions for the experiments with krypton were similar to the previous experiments (Figs. 7. and 8).

The krypton luminescence spectra consist mainly of KrI lines with all KrI lines belonging to the *5p-5s* transitions. The most intense lines are 769.4 nm, 819.0 nm, 826.3 nm and 829.8 nm. Emission intensity distribution of separate lines of krypton is presented in Table 3.

Table 3
Emission intensity distribution of separate lines of krypton

Wavelength measured, nm	Wavelength table, nm	Transition	0.3 s	1 s	3 s	10 s	Intensity, rel. units
557.6	557.3	2p1-1s4	04.	1.1	3.6	11.9	11.9
587.3	587.1	2p2-1s4	0.4	1.2	3.7	12	12
758.5	758.7	2p5-1s4	5.9	20.2	60.7	hv	202
760.8	760.1	2p6-1s5	41.4	hv	hv	hv	1380
769.7	769.4	2p7-1s5	3.3	11.1	33.9	hv	113
786	785.4	2p3-1s3	2.3	7.7	23.6	hv	78
806.6	805.9	2p4-1s3	1.1	3.8	12.2	40.4	40.4
811.8	811.2	2p9-1s5	22	hv	hv	hv	733
819.2	819.2	2p6-1s4	9.3	32.3	hv	hv	323
826.55	826.55	2p2-1s2	4.5	15.1	45.9	hv	153
830.22	830.22	2p10-1s5	10.9	37.4	hv	hv	374
851.50	851.50	2p4-1s2	1	3.1	9.8	32.9	32.9
877.81	877.81	2p8-1s4	4.5	15	47	hv	157
893.12	893.12	2p7-1s4	2.9	10	30.6	hv	102

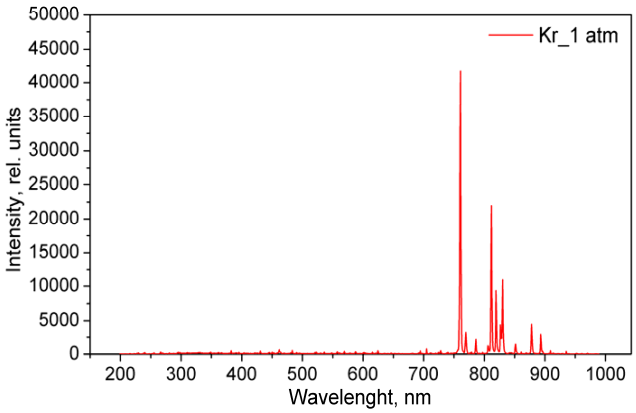

Fig. 7. Krypton emission spectrum at τ = 300 ms.

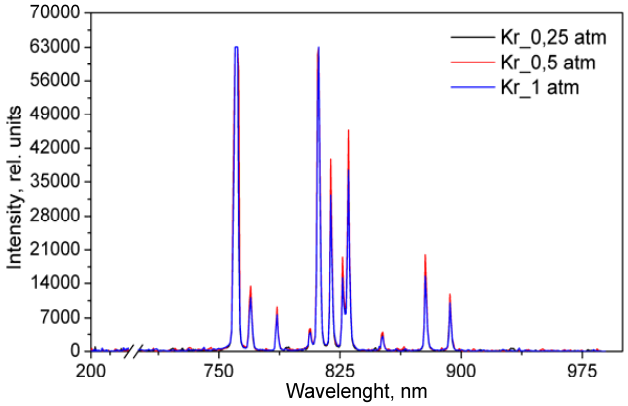

Fig. 8. Krypton emission spectrum at τ = 1 s.

Similar to the previous experiments, there were the conducted experiments with xenon. The Figs. 9 and 10 show xenon luminescence spectra for different values of the integration time.

Emission intensity distribution of separate lines of xenon is presented in Table 4.

It is worth to note that the continuum of krypton and xenon in the UV zone was limited to the transmission of the optical fiber.

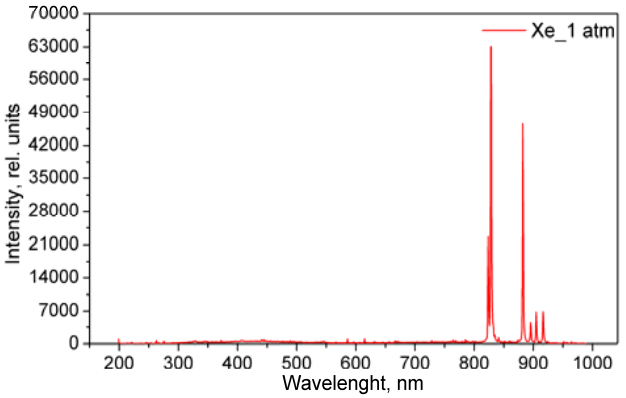

Fig. 9. Xenon emission spectrum at τ = 300 ms.

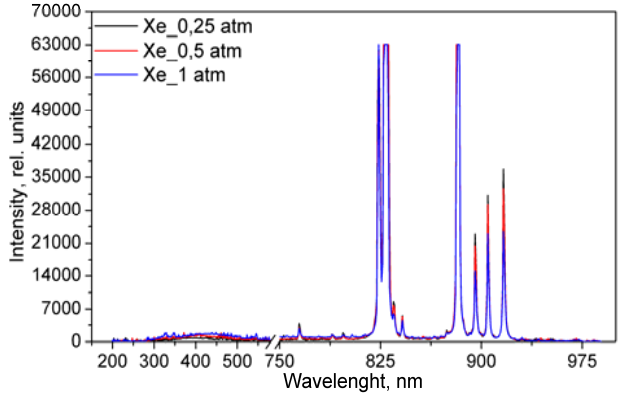

Fig. 10. Xenon emission spectrum at τ = 1 s.

Table 4
Emission intensity distribution of separate lines of xenon

Wavelength measured, nm	Wavelength table, nm	Transition	0.1 s	0.3 s	1 s	3 s	10 s	Intensity, rel. units
467.9	467.1	6s-7p	0.2	0.5	2	6	20	20
764.5	764.2	2p2-1s3	0.2	0.8	2.4	7.3	24.3	24.3
788.9	788.7	2p1-1s2	0.1	0.4	1.4	4.2	14.5	14.5
823.6	823.1	2p6-1s5	7.5	22.7	hv	hv	hv	757
826.5	826.6	2p2-1s2	1.6	5.7	16.7	50.2	hv	167
828.0	828.0	2p5-1s4	24.9	hv	hv	hv	hv	2490
834.6	834.6	2p3-1s2	0.8	1.8	6.1	18.6	hv	62
841.2	840.9	2p7-1s5	0.5	1.3	4.4	13.5	46.2	46.2
874.1	873.9	6d-6p	0.1	0.7	2	5.5	18.1	18.1
882.1	881.9	2p8-1s5	15.5	46.7	hv	hv	hv	1557
895.3	895.2	2p6-1s4	1.5	4.5	15.1	45.4	hv	151
904.7	904.5	2p9-1s5	2.3	6.8	22.9	hv	hv	229
916.3	916.2	2p7-1s4	2.3	6.9	23.6	hv	hv	236

3.2. The results of experiments with a binary Kr-Xe gaseous mixture

Molecular bands in the emission spectra of paired noble gases mixtures were first discovered more than half a century ago. In [11] high efficiency of $(ArXe)^+$, $(KrXe)^+$ luminescence, pumped by ionizing radiation is noted. In [12] KrXe mixture was excited by the products of $^3He(n,\alpha)T$ nuclear reaction in the central channel of the WWR-K reactor core with a flux of thermal neutrons of $(0.3\div1.0)\cdot10^{13}$ n/(cm^{2}s).

High selectivity of excitation of 491 nm band in Kr-Xe mixture in combined with absence of stable chemical compounds during irradiation and the ability to work at high temperatures indicate the prospect of using as a powerful nuclear-excited source of optical radiation. The 491 nm band is interesting in terms of creating detectors of ionizing radiation, as well as the output of light energy from a nuclear reactor core.

In the experiments with a binary krypton-xenon gaseous mixture, two reactor experiments with different concentrations of the constituent gaseous mixtures: Kr (0.005 atm) – Xe (1 atm) and Kr (0.5 atm) – Xe (0.5 atm) were conducted. Figure 11 shows the emission spectrum of the krypton-xenon gaseous mixtures at the thermal power of the IVG.1M reactor 6 MW at various pressure concentrations.

As can be seen from Fig. 11, a broad molecular band (band group) is observed in the range of 465–500 nm with a maximum wavelength of 491 nm.

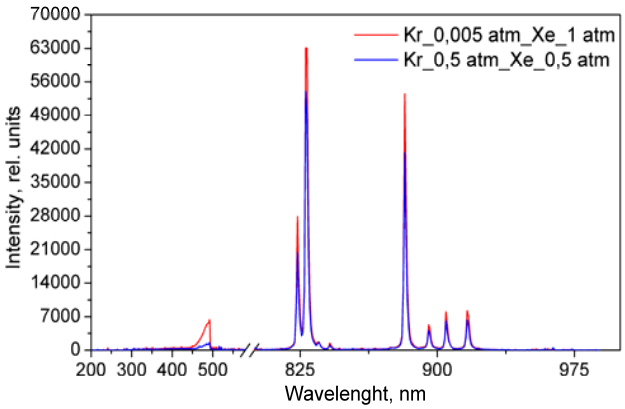

Fig. 11. The emission spectrum of a krypton-xenon mixture at τ = 300 ms.

In [13] the Kr-Xe gaseous mixture ratio was approximately 31:1. Molecular bands observed in the emission spectra of paired mixtures of noble gases excited by an electron beam were identified [14] as transitions between states of heteronuclear ionic molecules:

$$M + N \rightarrow (MN)^+ + h\nu$$

where the M^+N molecular states asymptotically correspond to the states of M^+N and the states of MN^+. $M + N^+$; here M. N – the atoms of noble gases, where N is the heavier atom.

Emission intensity distribution of separate lines of krypton-xenon gaseous mixture in the wavelength range from 200 nm up to 975 nm is presented in Table 5.

Table 5
Emission intensity distribution of separate lines of krypton-xenon gaseous mixture

Concentrations of the gaseous mixtures	Wavelength measured, nm	Wavelength table, nm	Transition	0.3s	1s	3s	10s	Intensity, rel. units
Kr (0.5 atm) – Xe (0.5 atm)	491.8	491	Molecular band	1.6	5.5	17.6	hv	58.7
Kr (0.005 atm) – Xe (1 atm)	491.8	491	Molecular band	7.1	20.8	54.8	hv	183
Kr (0.5 atm) – Xe (0.5 atm)	764.5	764.2	2p2-1s3	0.5	1.6	4.9	17.9	17.9
Kr (0.005 atm) – Xe (1 atm)				0.7	2.1	6.5	22.3	22.3
Kr (0.5 atm) – Xe (0.5 atm)	788.9	788.2	2p1-1s2	0.3	0.8	3	8.3	8.3
Kr (0.005 atm) – Xe (1 atm)				0.3	1.2	3.2	11.2	11.2
Kr (0.5 atm) – Xe (0.5 atm)	797.1	796.7	7p-6s	0.3	0.9	2.3	7.8	7.8
Kr (0.005 atm) – Xe (1 atm)				0.3	1	3.3	11.7	11.7
Kr (0.5 atm) – Xe (0.5 atm)	823.6	823.2	2p6-1s5	20.4	hv	hv	hv	680
Kr (0.005 atm) – Xe (1 atm)				27.8	hv	hv	hv	927
Kr (0.5 atm) – Xe (0.5 atm)	828	828	2p5-1s4	54	hv	hv	hv	1800
Kr (0.005 atm) – Xe (1 atm)				59.6	hv	hv	hv	1987
Kr (0.5 atm) – Xe (0.5 atm)	834.6	834.7	2p3-1s2	1.4	4.6	13.7	hv	45.7
Kr (0.005 atm) – Xe (1 atm)				1.8	5.8	17.9	hv	59.7
Kr (0.5 atm) – Xe (0.5 atm)	841.2	840.9	2p7-1s5	1.1	3.8	11.7	39.9	39.9
Kr (0.005 atm) – Xe (1 atm)				1.6	4.9	15	50.7	50.7
Kr (0.5 atm) – Xe (0.5 atm)	874.2	873.9	6d-6p	0.4	1.5	4.7	15.1	15.1
Kr (0.005 atm) – Xe (1 atm)				0.6	2.2	5.7	19.7	19.7
Kr (0.5 atm) – Xe (0.5 atm)	882.2	881.9	2p8-1s5	41	1.5	4.7	15.1	1367
Kr (0.005 atm) – Xe (1 atm)				53.3	hv	hv	hv	1777
Kr (0.5 atm) – Xe (0.5 atm)	895.3	895.2	2p6-1s4	4.1	14.1	42.5	hv	141
Kr (0.005 atm) – Xe (1 atm)				5.3	18.3	52.3	hv	174
Kr (0.5 atm) – Xe (0.5 atm)	904.8	904.5	2p9-1s5	6.2	21.1	hv	hv	211
Kr (0.005 atm) – Xe (1 atm)				8.2	27	hv	hv	270
Kr (0.5 atm) – Xe (0.5 atm)	916.4	916.3	2p7-1s4	6.4	22	hv	hv	220
Kr (0.005 atm) – Xe (1 atm				8.4	27.8	hv	hv	278

A band of heteronuclear ionic molecules of noble gases excited by electron and ion beams [15, 16] are weakly expressed in comparison with excitation by decay products.

4. Conclusions

In the course of this work, a series of experiments on research of emission characteristics of the single-component noble gases and the binary Kr-Xe mixture induced by products of ^{6}Li(n,α)T nuclear reaction was conducted in the stationary field of the IVG.1M reactor. As a result of the carried-out experiments, luminescent spectra of unary (Ne, Ar, Kr, Xe) and binary (Kr-Xe) gas mixture were measured and identified.

Reactor experiments with gaseous mixtures have shown the possibility of experiments to study the luminescence spectra of gaseous mixtures excited by the products of the nuclear reaction of ^{6}Li(n.α)T. The linear proportional dependence of thermal energy as compared with thermal neutron flux is noted.

Acknowledgments

This work was supported by the Ministry of Energy of the Republic of Kazakhstan within the framework of the agreement No. 71 on the theme «Development of nuclear energy in the Republic of Kazakhstan for the 2018-2020 years».

References

[1]. E.G. Batyrbekov, *Laser Part. Beams* 31 (2013) 637–687. DOI: 10.1017/S0263034613000098

[2]. M.U. Khasenov, *Laser Part. Beams* 32 (2014) 501–508. DOI: 10.1017/S0263034614000457

[3]. A.O. Sadvakassova, I.L. Tazhibayeva, E.A. Kenzhin, Zh.A. Zaurbekova, T.V. Kulsartov, Yu.N. Gordiyenko, Ye.V. Chikhray, *Fusion Sci. Technol.* 60 (2011) 9–15. DOI: 10.13182/FST11-A12398

[4]. Yu.N. Gordienko, T.V. Kulsartov, Zh.A. Zaurbekova, Yu.V. Ponkratov, V.S. Gnyrya, N.N. Nikitenkov. Bulletin of the Tomsk Polytechnic University [*Vestnik Tomskogo politehnicheskogo universiteta*] 324 (2014) 149–162 (in Russian).

[5]. N.A. Nazarbayev, V.S. Shkolnik, E.G. Batyrbekov, S.A. Berezin, S.N. Lukashenko, M.K. Skakov. Scientific, Technical and Engineering Works to Ensure the Safety of the Former Semipalatinsk Test Site. Vol. 3 (2017) 596 p.

[6]. E.G. Batyrbekov, Yu.N. Gordienko, Yu.V. Ponkratov, M.U. Khasenov, I.L. Tazhibayeva, N.I. Barsukov, T.V. Kulsartov, Zh.A. Zaurbekova, Ye.Yu. Tulubayev, M.K. Skakov, *Fusion Eng. Des.* 117 (2017) 204–207. DOI: 10.1016/j.fusengdes.2016.06.055

[7]. Yu.N. Gordienko, E.G. Batyrbekov, M.U. Khasenov, Zh.A. Zaurbekova, Yu.V. Ponkratov, T.V. Kulsartov, N.I. Barsukov, Ye.Yu. Tulubayev, A.O. Mukanova, *Materials Today: proceedings* 4 (2017) 4589–4598. DOI: 10.1016/j.matpr.2017.04.034

[8]. E.G. Batyrbekov, Yu.N. Gordienko, N.I. Barsukov, Yu.V. Ponkratov, T.V. Kulsartov, M.U. Khassenov, Zh.A. Zaurbekova, Ye.Yu. Tulubayev, K.K. Samarkhanov, Proceedings Volume 10614, International Conference on Atomic and Molecular Pulsed Lasers XIII; 106141K (2018). DOI: 10.1117/12.2303578

[9]. G.A. Batyrbekov, E.G. Batyrbekov, V.A. Danilychev, M.U. Khasenov, *Soviet Journal of Quantum Electronics* 20 (1990) 1084–1088. DOI: 10.1070/QE1990v020n09ABEH007409

[10]. A.A. Abramov, V.V. Gorbunov, S.P. Melnikov, A.Kh. Mukhamatullin, A.A. Pikulev, A.V. Sinitsyn, A.A. Sinyanskii, V.M. Tsvetkov, Proceedings Volume 6263, Atomic and Molecular Pulsed Lasers VI; 626312 (2006) P. 279–296. DOI: 10.1117/12.677457

[11]. M.U. Khasenov, Proceedings Volume 6263, Atomic and Molecular Pulsed Lasers VI; 626314 (2006). DOI: 10.1117/12.677459

[12]. M.U. Khasenov, *J. Appl. Spectrosc.* 72 (2005) 316–320. DOI: 10.1007/s10812-005-0076-7

[13]. W. Friedl, *Zeitschrift für Naturforschung A* 14 (1959) 848–848. DOI: 10.1515/zna-1959-0920

[14]. Y. Tanaka, K. Yoshino, D.E. Freeman, *J. Chem. Phys.* 62 (1975) 4484–4496. DOI: 10.1063/1.430356

[15]. Yu.N. Gordienko, M.U. Khasenov, E.G. Batyrbekov, A.K. Amrenov, K.K. Samarkhanov, Yu.V. Ponkratov, *Appl. Spectrosc.* 85 (2018) 600–604. DOI: 10.1007/s10812-018-0692-7

[16]. M.U. Khasenov, *Laser Part. Beams* 34 (2016) 655–662. DOI:10.1017/S0263034616000616